AD-A059 918 SCIENCE APPLICATIONS INC SUNNYVALE CALIF F/G 13/11
FEASIBILITY STUDY FOR PERFORMING AN X-RAY ATTENUATION MEASUREME--ETC(U)
MAR 78 R I MILLER DNA001-77-C-0158
UNCLASSIFIED SAI-78-506-SV DNA-4466F NL

END
DATE FILMED
12-78
DDC

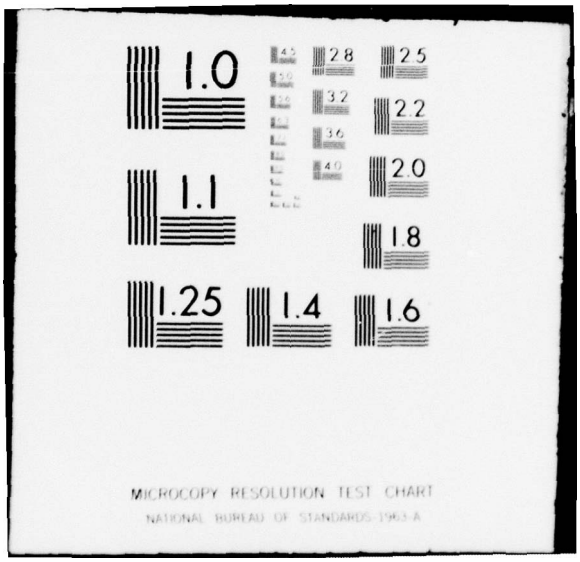
1.0
1.1
1.25
1.4
1.6
2.8
3.2
3.6
4.0
2.5
2.2
2.0
1.8
MICROCOPY RESOLUTION TEST CHART
NATIONAL BUREAU OF STANDARDS-1963-A

LEVEL II

DNA 4466F

FEASIBILITY STUDY FOR PERFORMING AN X-RAY ATTENUATION MEASUREMENT

Science Application, Incorporated
1257 Tasman Drive
Sunnyvale, California 94086

31 March 1978

Final Report for Period 1 February 1977—28 February 1978

CONTRACT No. DNA 001-77-C-0158

APPROVED FOR PUBLIC RELEASE;
DISTRIBUTION UNLIMITED.

THIS WORK SPONSORED BY THE DEFENSE NUCLEAR AGENCY
UNDER RDT&E RMSS CODE B344077462 J34GAXSX35503 H2590D.

Prepared for
Director
DEFENSE NUCLEAR AGENCY
Washington, D. C. 20305

Destroy this report when it is no longer needed. Do not return to sender.

PLEASE NOTIFY THE DEFENSE NUCLEAR AGENCY, ATTN: TISI, WASHINGTON, D.C. 20305, IF YOUR ADDRESS IS INCORRECT, IF YOU WISH TO BE DELETED FROM THE DISTRIBUTION LIST, OR IF THE ADDRESSEE IS NO LONGER EMPLOYED BY YOUR ORGANIZATION.

(18) DNA, SBIE

UNCLASSIFIED

SECURITY CLASSIFICATION OF THIS PAGE (When Data Entered)

REPORT DOCUMENTATION PAGE

READ INSTRUCTIONS BEFORE COMPLETING FORM

(19)

1. REPORT NUMBER: DNA 4466F, AD-E300 334
2. GOVT ACCESSION NO.
3. RECIPIENT'S CATALOG NUMBER

4. TITLE (and Subtitle): (10) FEASIBILITY STUDY FOR PERFORMING AN X-RAY ATTENUATION MEASUREMENT.

5. TYPE OF REPORT & PERIOD COVERED: (9) Final Report, for Period 1 Feb 77—28 Feb 78

6. PERFORMING ORG. REPORT NUMBER: (14) SAI-78-506-SV

7. AUTHOR(s): (10) R. I. Miller

8. CONTRACT OR GRANT NUMBER(s): (15) DNA 001-77-C-0158

9. PERFORMING ORGANIZATION NAME AND ADDRESS:
Science Applications, Incorporated
1257 Tasman Drive
Sunnyvale, California 94086

10. PROGRAM ELEMENT, PROJECT, TASK AREA & WORK UNIT NUMBERS:
Subtask J34GAXSX355-03

11. CONTROLLING OFFICE NAME AND ADDRESS:
Director
Defense Nuclear Agency
Washington, D.C. 20305

12. REPORT DATE: (11) 31 March 1978

13. NUMBER OF PAGES: 52

14. MONITORING AGENCY NAME & ADDRESS (if different from Controlling Office)

15. SECURITY CLASS (of this report): UNCLASSIFIED

15a. DECLASSIFICATION/DOWNGRADING SCHEDULE

16. DISTRIBUTION STATEMENT (of this Report)

Approved for public release; distribution unlimited.

(12) 52 p. (16) J34GAXS (17) X355

17. DISTRIBUTION STATEMENT (of the abstract entered in Block 20, if different from Report)

18. SUPPLEMENTARY NOTES

This work sponsored by the Defense Nuclear Agency under RDT&E RMSS Code B344077462 J34GAXSX35503 H2590D.

19. KEY WORDS (Continue on reverse side if necessary and identify by block number)

X-ray Transmission
X-ray Attenuation
Air Shock

20. ABSTRACT (Continue on reverse side if necessary and identify by block number)

SAI has investigated the feasibility of performing an x-ray attenuation measurement to determine the time-dependent density and composition of material in a pipe through which a multikilobar air shock is driven. A flash x-ray system will be able to generate adequate signal levels in direct viewing solid state detectors and in scintillator-photomultipliers observing irradiated fluorescers. The major problem is the design of a line-of-sight protection system which can adequately withstand kilobar pressures. A

DD FORM 1 JAN 73 1473 EDITION OF 1 NOV 65 IS OBSOLETE

UNCLASSIFIED

SECURITY CLASSIFICATION OF THIS PAGE (When Data Entered)

390 383

20. ABSTRACT (Continued)

minimal experimental effort on Hybla Gold verified both adequately low background levels and detector survivability for the required few milliseconds.

TABLE OF CONTENTS

LIST OF ILLUSTRATIONS

LIST OF TABLES

1. INTRODUCTION

SAI, in conjunction with SLA and RDA, has investigated the feasibility of performing an x-ray attenuation measurement to determine the time-dependent density and composition of material in a shock-driven pipe. In the Hybla Gold nuclear underground test, shock fronts with initial pressures as high as 50 kbars were driven into concrete and steel pipes. The shock front moving down these pipes ablates material from their walls, so that at any given location the initial leading edge of the air shock quickly gives over to pipe debris. Figure 1.1 presents the predicted mass density profiles for air and concrete debris at 70 meters from the initiating pressure front in a three foot diameter concrete pipe. The peak shock pressure at this location was predicted to be about 6 kbars, down from 50 kbars at the head of the pipe. This report presents the results of a study undertaken to design an x-ray densitometer system to determine the time-dependent density and composition of the material in such a pipe and under such conditions.

The work was carried out in conjunction with a similar effort under the direction of Dr. Jacques Hoefelder of Sandia Laboratory, Albuquerque (SLA), who was involved in designing a similar experiment as part of the overall SLA effort on Hybla Gold. Dr. Morgan Grover of RDA also devoted a significant amount of his time to the conceptual design of the experiment and to coordinating the SLA and SAI efforts.

The initial stage of the study was concerned with defining an experimental system capable of determining the desired flow parameters. Typical of the various topics addressed were the following:

i) The characteristics required of an x-ray source adequate to generate observable signal levels for a few milliseconds.

ii) The design of a suitable x-ray detector system with response characteristics capable of determining both material density and composition.

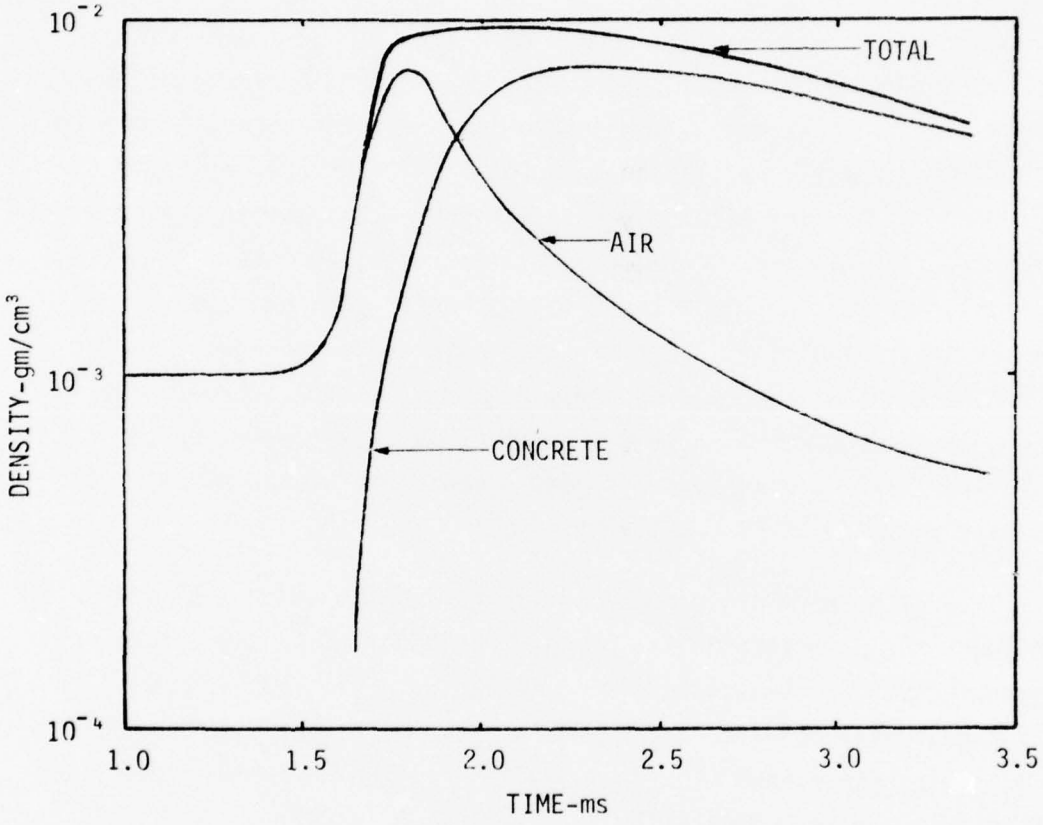

Figure 1.1. Material densities for shock wave driven through a 3 foot concrete pipe at 70 meters.

iii) The design of an x-ray line-of-sight system that would not perturb the pipe flow, not attenuate the x-ray beam, and survive the pressures generated in the pipe.

iv) The shielding and/or configuration necessary to reduce gamma, neutron and EMP induced background levels to less than the predicted signal levels.

In order to verify calculated background levels and detector survivability for the few milliseconds required, SAI fielded two x-ray detectors in a typical experimental configuration on the Hybla Gold event.

2. TECHNICAL DISCUSSION

2.1 General Problem

The x-ray densitometer system should be capable of determining shock flow conditions as shown in Figure 1.1. Table 2.1 lists narrow beam x-ray transmissions through one meter of air, concrete (ordinary and rock matching) and iron at densities of 10^{-1}, 10^{-2}, and 10^{-3} g/cm^3. To determine material densities in a one or three foot diameter pipe as used on Hybla Gold, the x-ray beam is assumed to traverse a pipe diameter through suitably transmitting x-ray windows in the pipe wall. Constraints on the minimum window thickness necessary to maintain pipe wall integrity during the shocked flow will place a lower limit on the x-ray energies that can be observed. For example, a 2 cm thickness of beryllium is only 10 percent transmitting at 10 keV, 35 percent transmitting at 15 keV and 55 percent transmitting at 50 keV. Since windows are required on either side of the pipe diameter, it is apparent that only energies above 15 keV can be transmitted effectively through the pipe walls. To distinguish air from concrete at densities of 10^{-3} to 10^{-2} g/cm^3, two separate x-ray transmission measurements at differing energies are required, one as low in energy as possible, around 20 keV, the other as high in energy as possible, above 50 keV.

These two energy bands must be obtained by combining an x-ray source with a sufficiently wide band or dual band output with a suitable x-ray detector system. Signal level constraints necessitate both as intense an x-ray source as possible and a very sensitive x-ray detection technique.

2.2 X-ray Generators

Commercially available x-ray generators direct a current of high energy electrons onto a suitable target to produce a bremsstrahlung

Table 2.1. Narrow Band X-Ray Transmission Through One Meter of Relevant Materials

Material density g/cm^3	Energy-keV							
	10	15	20	30	40	50	60	80
Air								
10^{-3}	.610	.857	.928	.966	.976	.980	.982	.984
10^{-2}	.007	.214	.475	.710	.784	.815	.830	.847
10^{-1}	--	--	.001	.033	.088	.129	.156	.190
Ordinary Concrete[1]								
10^{-3}	.070	.438	.698	.889	.942	.962	.971	.979
10^{-2}	--	--	.027	.307	.553	.681	.748	.810
10^{-1}	--	--	--	--	.003	.021	.055	.122
Rock Matching Concrete[2]								
10^{-3}	.005	.188	.453	.763	.589	.741	.827	.909
10^{-2}	--	--	--	.067	.005	.050	.150	.387
10^{-1}	--	--	--	--	--	--	--	--
Iron								
10^{-3}	--	.004	.083	.443	.696	.824	.888	.942
10^{-2}	--	--	--	--	.027	.143	.304	.552
10^{-1}	--	--	--	--	--	--	--	.003

[1]Composition by weight: .006H, .498 O, .017Na, .002Mg, .046Al, .316Si, .001S, .019K, .083Ca, .012Fe.

[2]Composition by weight: .03H, .53 O, .01Al, .12Si, .05S, .06Ca, .20Ba.

continuum of x-radiation with some few percent addition of characteristic radiation from the target material.[1] The bremsstrahlung power for submegavolt electrons is given roughly by[2]

$$P = 1.1 \times 10^{-9} V^2 IZ \qquad (2.1)$$

where P = the x-ray bremsstrahlung output in watts
V = the electron energy in volts
I = the electron current in amperes
Z = the anode atomic number.

X-ray machines are of three basic types:

a) 5 kW continuous mode water or oil cooled anode tubes with operating currents in the tens of milliampere range at 150 kV;

b) 100 kW pulsed mode tubes of liquid cooled or rotating anode design producing 100 ms wide pulses with current levels as high as a half ampere at 150 kV;

c) 500 MW field emission diodes producing 100 ns wide pulses with current levels of 2 to 5 kA at 150 kV.

The continuous mode x-ray generators are readily available from a number of manufacturers (Philips, Pickler, Machlett) and are limited in their output level to the power that can be dissipated in a water or oil cooled target. The low and intermediate level generators utilize a heated filament as their electron source. Filament sagging prevents generating

---

1. C.E. Dick, A.C. Lucas, J.N. Rotz, R.C. Placious, and J.N. Sparrow, Large Angle X-Ray Production by Electrons, J. Appl. Phys. 44, 2 (1973).

2. A.H. Compton and S.K. Allison, X-Rays in Theory and Experiment, D. Van Nostrand, (1935).

significantly higher current levels because of the close filament-anode spacing required for efficient operation. Stationary anode tubes can be pulsed at power levels of 30 kW, while rotating anode tubes can be pulsed at higher levels of 100 kW because of the increased anode area available to dissipate the heat load without physical damage. A charged capacitor bank is used for the power source, with a voltage drop of about 10 percent occurring in a few tens of milliseconds at full output.

In the most intense type of x-ray generator, the exciting electron current is produced by field emission from a conical cathode. The current level in such tubes is limited to the maximum current that can readily be carried by a coaxial cable. Hewlett-Packard presently manufactures the FEMCO flash x-ray system utilizing a single HV cable. Physics International (PI) has built a similar flash x-ray system (COBRA) utilizing three HV cables for increased yield, but this generator is not in commercial production. Since the flash x-ray system cannot be recharged and refired on the millisecond time scale required, a number of such generators would have to be fired sequentially every few tenths of a millisecond to obtain a series of 50 to 100 ns snapshots of the shocked flow.

All three types of x-ray generator require running a 150 kV coaxial cable from a high voltage DC or capacitor bank power source and control unit to a reasonably compact x-ray head. Fielding such a system underground would require careful design but should not present any insurmountable problems.

The cost of a continuous anode system is about 20K; the cost of a rotating anode system is about 35K; the cost of an array of six flash x-ray generators would be about 50K.

Even with the most sensitive x-ray detection system that can be fielded in a UGT environment, as will be discussed in the next section, signal levels on the order of milliamperes are all that can be obtained with the flash x-ray system, microamperes from the pulsed x-ray system and nanoamperes from the continuous x-ray system. The flash x-ray system thus offers the maximum chance of obtaining signal levels that can be readily resolved from neutron and gamma induced background, as well as from EMP levels and DC offsets affecting the late-time recording of the data. The additional effort to fire sequentially a number of such tubes over a period of a few milliseconds is judged to be not prohibitive and readily justified by the increased signal levels.

Figure 2.1 presents the calculated spectral output of a Hewlett-Packard Model 4373A Flash X-ray System run at 170kV, 2kA and employing a tungsten anode and 25 mil thick beryllium window for maximum bremsstrahlung output. The total output of 1.0 MW is a factor of 5 less than the output predicted from Eq. 2.1, primarily because of source geometry and absorption effects in the x-ray anode and window assemblies. In addition to the bremsstrahlung output, about 6 percent additional radiation comes out in the tungsten K lines at 60 keV.

The flash x-ray tube can also be made with a molybdenum anode. The bremsstrahlung output of this tube is about half that of the tungsten anode tube, but the output intensity in the characteristic molybdenum K lines at 17.8 keV is 5 times larger, being about 60 percent of the total bremsstrahlung output. A molybdenum anode tube could be used to enhance the x-radiation required to make a low energy transmission measurement below 20 keV. Figure 2.2 presents the calculated spectral output of a Model 5296 flash x-ray system run at 150 kV and 2 kA and employing a molybdenum anode and 25 mil thick beryllium window.

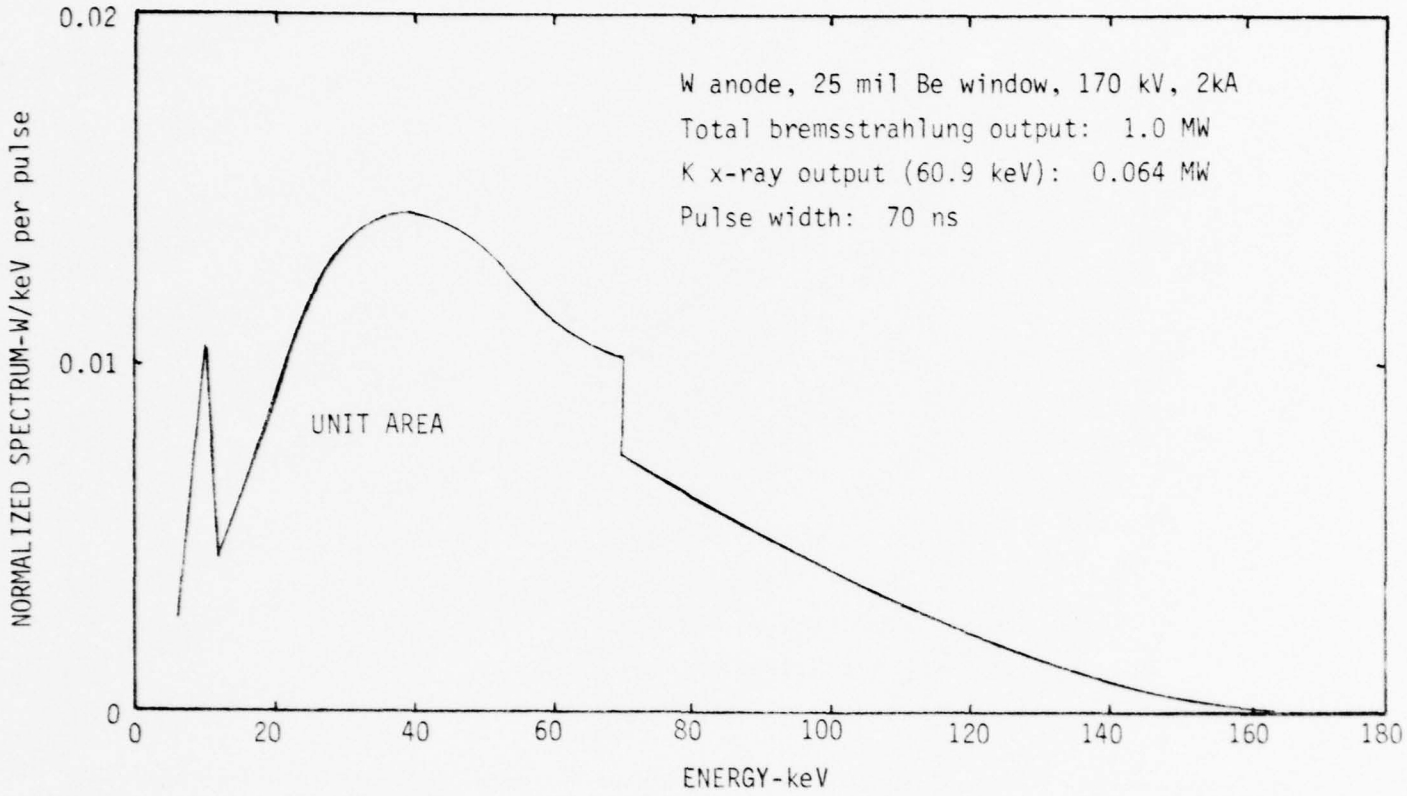

Figure 2.1. Calculated output of tungsten anode flash x-ray system.

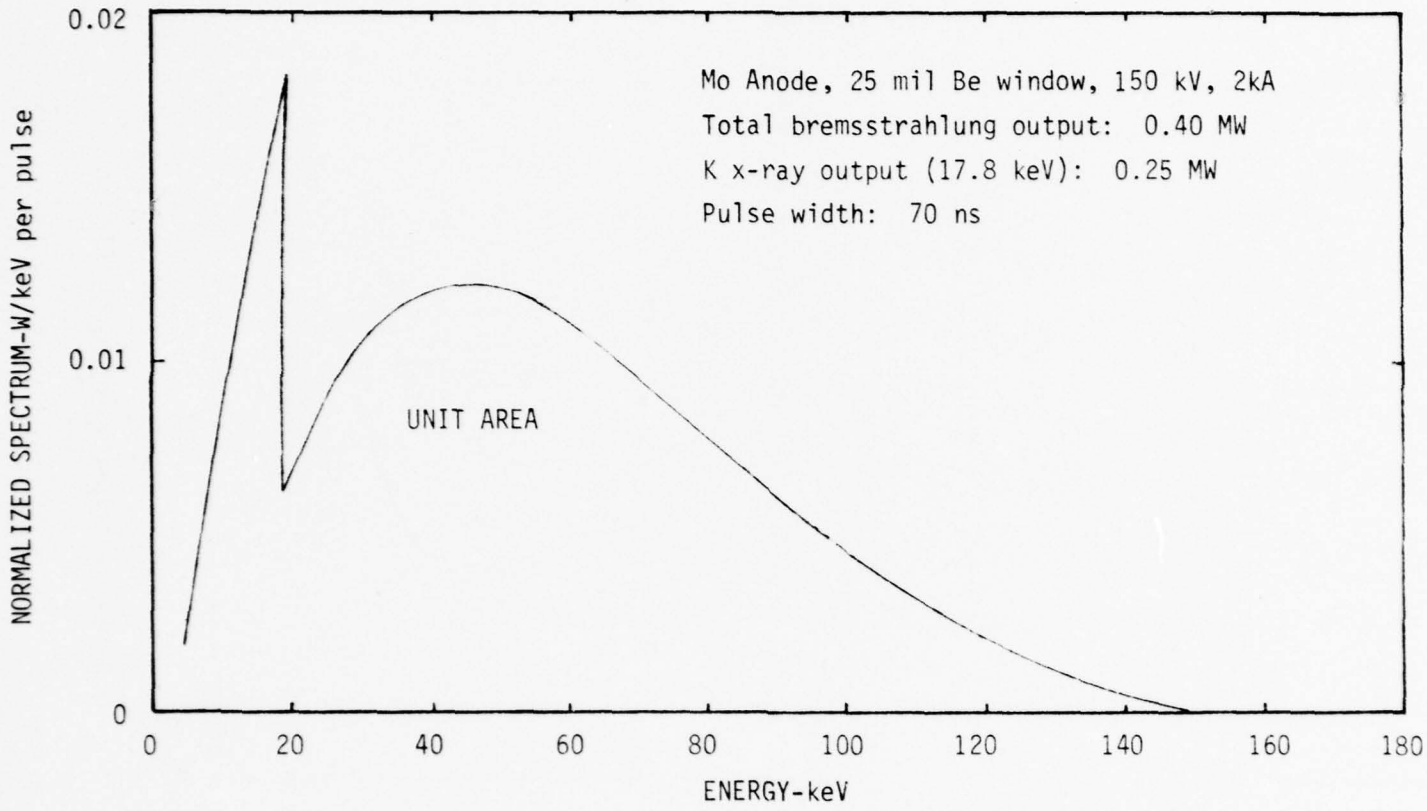

Figure 2.2. Calculated output of molybdenum anode flash x-ray system.

2.3 X-ray Detection Techniques

In order to distinguish shocked air from ablated wall material, two transmission measurements are required. A high energy measurement is required to determine the total mass in the line-of-sight, independent of the elemental composition, since at sufficiently high energy all materials attenuate x-radiation by Compton electron scattering which is dependent only on the total number of electrons. At low energies, materials interact with x-rays primarily through photoelectric absorption which is strongly dependent on atomic number. For air, Compton and photoelectric absorption are comparable at 30 keV; for ordinary concrete containing primarily oxygen, silicon and calcium, at 50 keV; for rock matching concrete containing an additional 20 percent barium by weight, at 150 keV; for iron, at 100 keV. Figure 2.3 presents absorption coefficients for the above materials and also the corresponding transmission through a one meter path of material at 10^{-2} g/cm^3 density.

Two transmission measurements are required to determine both total areal density and material composition: one measurement at a sufficiently high energy that all attenuation is essentially through Compton scattering, one measurement at a sufficiently low energy that the photoelectric attenuation is indicative of the atomic number of the attenuating material.

In a two transmission measurement to determine density and composition, the equations for the measured transmissions, T and T', are given by

$$\ln T = \mu_1 X_1 + \mu_2 X_2 \qquad (2.2a)$$

$$\ln T' = \mu_1' X_1 + \mu_2' X_2 \qquad (2.2b)$$

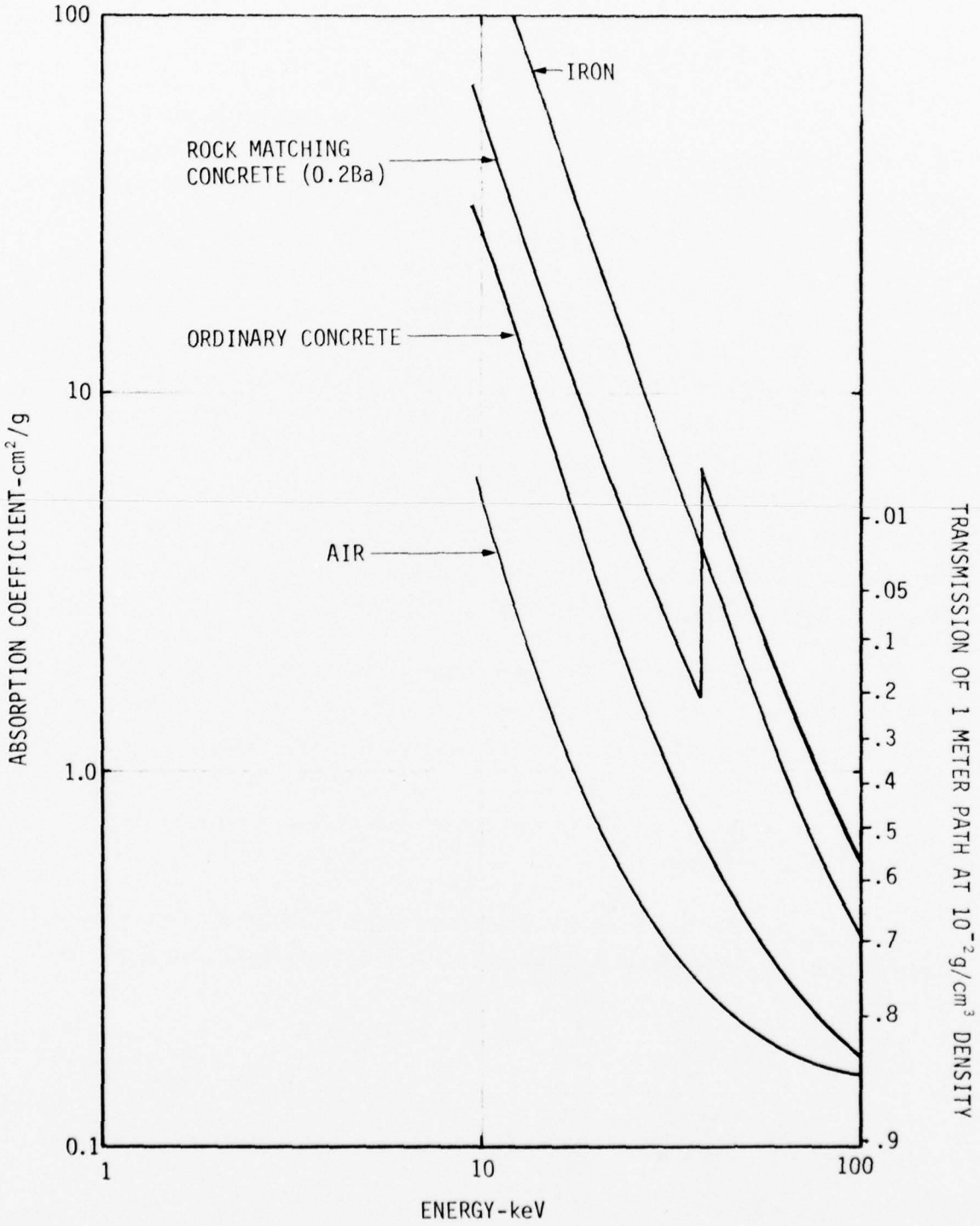

Figure 2.3. Absorption coefficients and transmissions for materials in shocked pipe.

where X_1 and X_2 are the areal densities of the two materials in the x-ray beam, μ_1 and μ_2 are their respective absorption coefficients, and the unprimed and primed quantities refer to the average energies E and E', at which the separate transmission measurements are performed.

At energies sufficiently great that Compton scattering dominates photoelectronic absorption, $\mu_1 \simeq \mu_2 \simeq \mu_C$, where μ_C is the total Compton cross section, so that the total areal density in the beam, $X_1 + X_2$, is given by

$$(X_1 + X_2) = \ln T/\mu_C \tag{2.3}$$

In general, however,

$$X_1 + X_2 R = \ln T/\mu_1 \tag{2.4a}$$

$$X_2 + X_2 R' = \ln T'/\mu_1' \tag{2.4b}$$

where $R = \mu_2/\mu_1$, $R' = \mu_2'/\mu_1'$. These equations are readily solved to yield the results:

$$X_1 = \frac{\ln T/\mu_1 - \ln T'/\mu_1'}{R - R'} \tag{2.5}$$

In order that these equations have well defined solutions, we require:

i) $R/R' \neq 1$

ii) $\ln T$, $\ln T'$ well determined.

The requirement that $R/R' \neq 1$ imposes constraints on the energy bands in which the transmission measurements should be made. For example, for $E \simeq 30$ keV and $E' \simeq 70$ keV, $R/R' \simeq 2$ for discriminating air from concrete, but $R/R' = 1$ for discriminating air from rock matching grout (0.2 Ba).

The accuracy of the transmission measurement is expected to be about 5 percent for transmissions between 1 and 0.2. It is not

anticipated that either signal level magnitude or the dynamic range of the recording system will allow transmissions less than 0.01 to be determined. These uncertainites in $\Delta T/T$,

$$\Delta T/T \simeq 0.05 \qquad (1 > T > 0.2)$$
$$\Delta T/T = 0.01/T \qquad (0.2 > T > 0.01)$$
$$T \text{ undefined} \qquad (T < 0.01)$$

can be used to estimate the uncertainty in $\ln T$ through the approximation

$$\ln(T + \Delta T) \simeq \ln T + \Delta T/T \qquad (2.6)$$

so that

$$\frac{\Delta \ln T}{\ln T} \simeq \frac{\Delta T/T}{\ln T} \qquad (2.7)$$

This quantity is graphically presented in Figure 2.4 as a function of T for the assured uncertainty in the determination of $\Delta T/T$. Transmissions from 0.01 to 0.8 will be required for determining the areal densities X_1 and X_2 with better than 20 percent accuracy.

Two high sensitivity x-ray detection techniques are suitable for observing the x-radiation from the x-ray generator. Figure 2.5 presents a conceptual layout of both detection techniques. In the first and simpler, a silicon solid state detector (SSD) observes the x-ray source directly, possibly through a band defining K-edge filter. Silicon is the x-ray absorbing element in such a detector and the detector thickness is typically on the order of 1 mm. As a result, the detector becomes increasingly transparent to radiation higher in energy than 20 keV and hence is suitable only for the lower energy transmission measurement.

The alternative x-ray detection technique utilizes a scintillator coupled to a high gain photomultiplier to observe the K fluorescence from elemental materials placed in the x-ray beam. The fluorescer photoelectrically

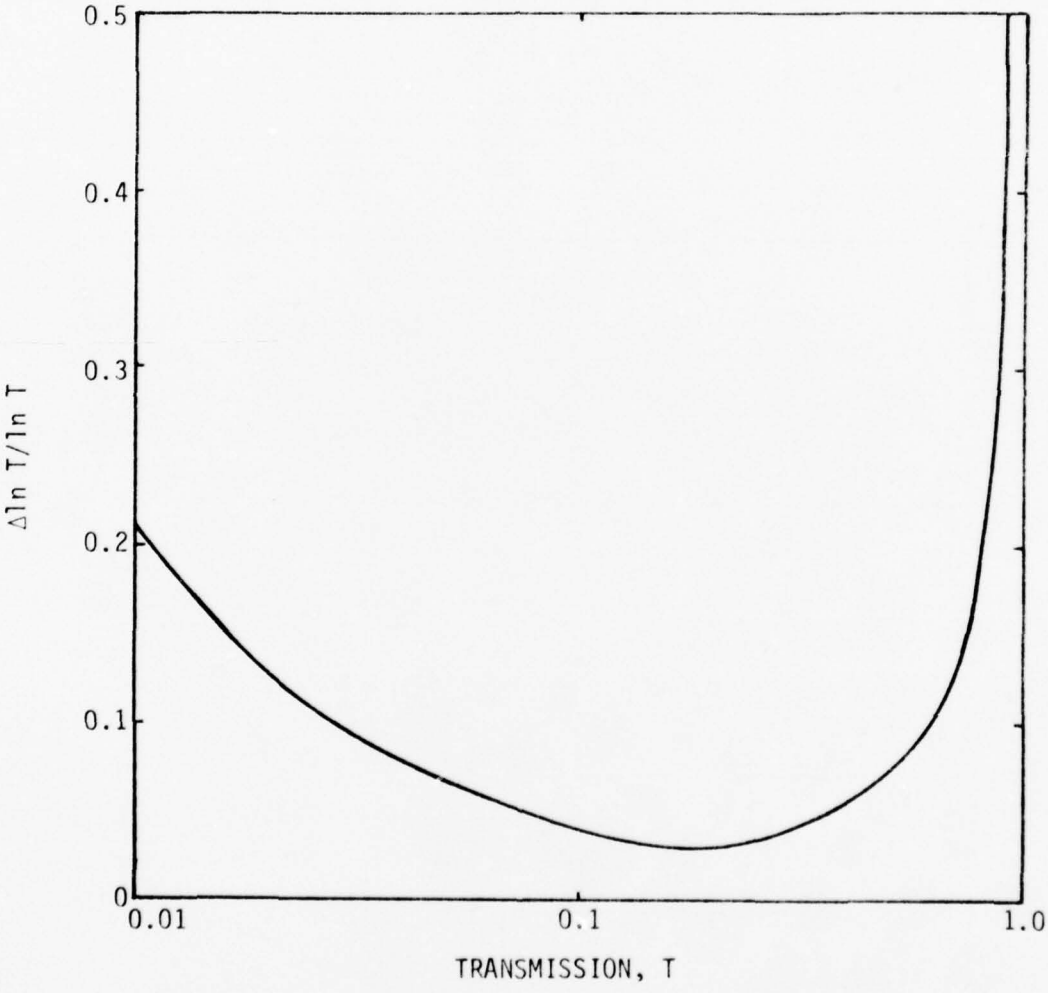

Figure 2.4. Uncertainty in ln T as a function of transmission, T.

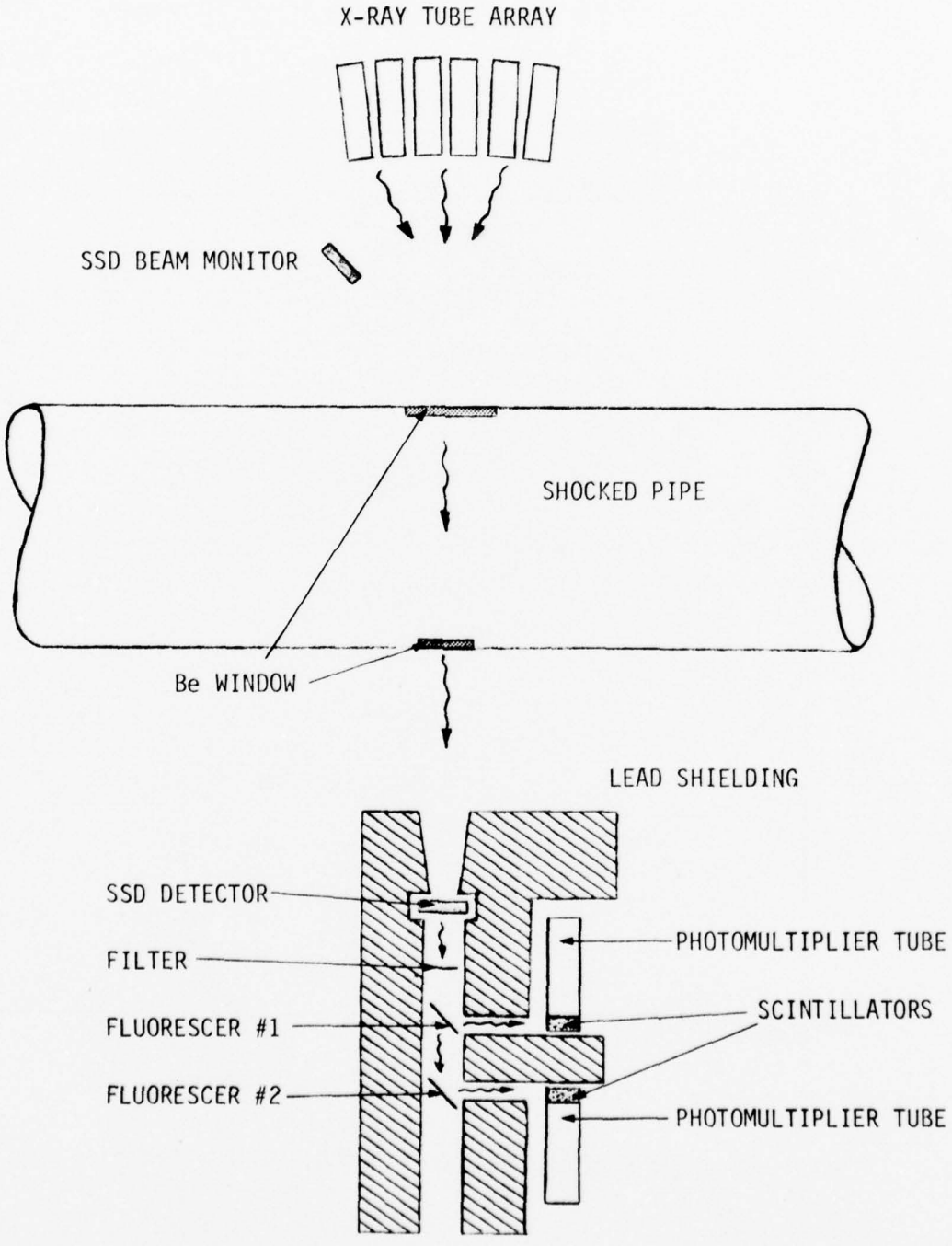

Figure 2.5. Conceptual layout of x-ray transmission measurement experiment.

absorbs photons with energy greater than its K-edge energy and characteristic K x-rays are emitted when the K-shell electron vacancy is filled by an L-shell electron. The fluorescent radiation can then be measured by a suitably collimated x-ray detector, in this instance a scintillator to generate a light pulse from the incident K fluorescence and a photomultiplier tube to convert this light pulse into a measurable electron current. To obtain additional energy resolution, an elemental filter with a K edge slightly higher in energy than the fluorescer K edge can be used to preferentially transmit to the fluorescer those x-rays that fall in the region of relatively low absorption just below the filter K-absorption edge. In this way, a filter-fluorescer channel can be obtained with response peaked between the filter and fluorescer K edges.

The fluorescer/scintillator-photomultiplier channels can observe average energies as low as about 30 keV with a molybdenum fluorescer (K edge energy of 20 keV), as high as 70 keV with an erbium fluorescer (K edge energy of 57.5 keV). Higher energy channels are not necessary for distinguishing air from concrete since both materials absorb x-rays by Compton rather than photoelectric absorption above 50 keV.

In Figure 2.5 two fluorescer channels are indicated as being fielded in a common line-of-sight with an unfiltered solid state detector channel. This configuration for the three channels is readily realized with no significant penalty in channel response, since the in-beam components in the preceeding lower energy channels can be designed adequately thin that they are essentailly transparent to the x-rays being measured by the higher energy channels fielded behind them. The solid state detector is mounted in a transmission mount so that only the silicon disc is in the collimated line-of-sight. In this fashion, a significant savings can be accomplished in the design of the line-of-sight system, since only one pair of x-ray transmitting windows is required to provide x-ray transmission through the pipe walls.

Figure 2.6 presents the response functions for an unfiltered 300μm thick SSD, a 20 mg/cm^2 molybdenum fluorescer filtered by 50 mg/cm^2 of Sn and fielded behind the SSD, and a 200 mg/cm^2 erbium fluorescer fielded behind the molybdenum fluorescer. The x-ray source is assumed to be three meters from a 5 cm^2 collimator defining both the irradiated SSD area and the irradiated fluorescer area. The scintillators are assumed to have a collimated area of 5 cm^2 and to be 30 cm from the fluorescer. The combined x-ray sensitivity of the scintillator-photomultiplier combination is assumed to be 10^2 coulombs/joule of incident x-rays, corresponding to a 10^6 gain photomultiplier coupled to a lead or tin loaded plastic scintillator (NE-102 or Pilot B). The three meter source-detector distance allows a one meter separation for both source and detectors from the walls of a one meter diameter pipe; the 30 cm fluorescer-scintillator distance allows adequate shielding of the photomultiplier tube; the photomultiplier tube is placed at right angles to the fluorescer-scintillator axis to allow further neutron and gamma shielding, as will be discussed in Section 2.5. The x-ray transmitting windows on either side of the shock driven pipe are each assumed to be one inch thick, as will be discussed in Section 2.4. The sensitivity of the silicon SSD is 0.272 coulombs/joule of absorbed energy, corresponding to a value of 3.67 ev to create an electron-hole pair in silicon. All the above assumed values are typical of a realistic experimental configuration.

With a tungsten anode x-ray source operating at 170 kV, 2 kA and producing 1.0 MW of x-rays into 4π steradians as presented in Figure 2.1, the calculated signal levels with no attenuating material in the pipe are approximately 10 mA for the unfiltered SSD channel, 5 mA for the molybdenum fluorescer channel and 20 mA for the erbium fluorescer channel. Table 2.1 lists attenuations in those signal levels for possible shocked materials over the range of density expected.

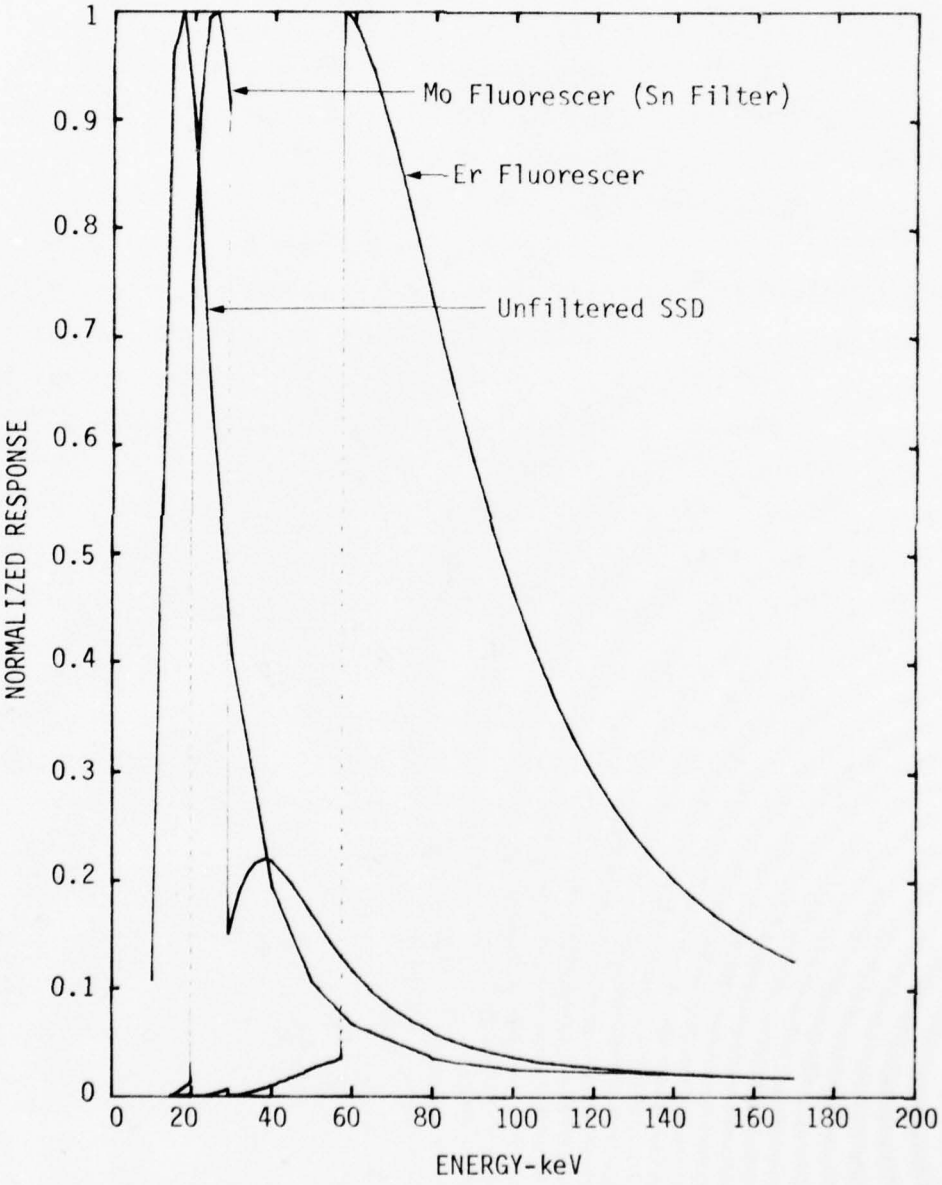

Figure 2.6. Response functions for typical x-ray transmission channels.

The unfiltered SSD channel observes an average energy of about 25 keV, lower energies being attenuated by the two inches of beryllium required for the x-ray windows, higher energies not being absorbed in the silicon detector. The lower energy tin-filtered molybdenum channel observes an average energy between 25 and 30 keV. Despite the fact that the molybdenum channel response function, as shown in Figure 2.6, peaks at an energy 5 to 10 keV higher than that for the SSD channel, when the respective response functions are folded with the tungsten source function presented in Figure 2.1, the average energy observed by these channels is not significantly different. Filtering the SSD channel or removing the filtering from the molybdenum fluorescer channel have minimal effect on the average energy observed. The erbium fluorescer channel observes an average energy between 60 to 70 keV, again relatively independent of the lack or presence of filters. Alternative fluorescers would provide transmission measurements at average energies about 25 percent greater than the fluorescer K edge energy, but molybdenum and erbium effectively span the range over which such measurements can be made with adequate signal levels.

Figures 2.7 and 2.8 present x-ray transmission as a function of air and concrete material density in a 1 meter pipe for the molybdenum and erbium fluorescer channels, respectively. The direct viewing solid state detector generates transmissions similar to those for the molybdenum channel. The anticipated uncertainty in the determination of lnT for transmissions greater than 0.8, as discussed previously, limit the accurate determination of air densities to those greater than about 5×10^{-3} g/cm^3. Nonetheless, these two channels would readily be able to distinguish shocked air from ablated wall material at the predicted 10^{-3} to 10^{-2} g/cm^2 densities as presented in Figure 1.1.

If a molybdenum anode flash x-ray system with about 0.5 MW x-ray output into 4π steradians is used as the x-ray source, unattenuated signal levels of approximately 15 mA are calculated for the unfiltered SSD channel, 2 MA for the molybdenum fluorescer channel, and 6 mA for the erbium fluorescer channel.

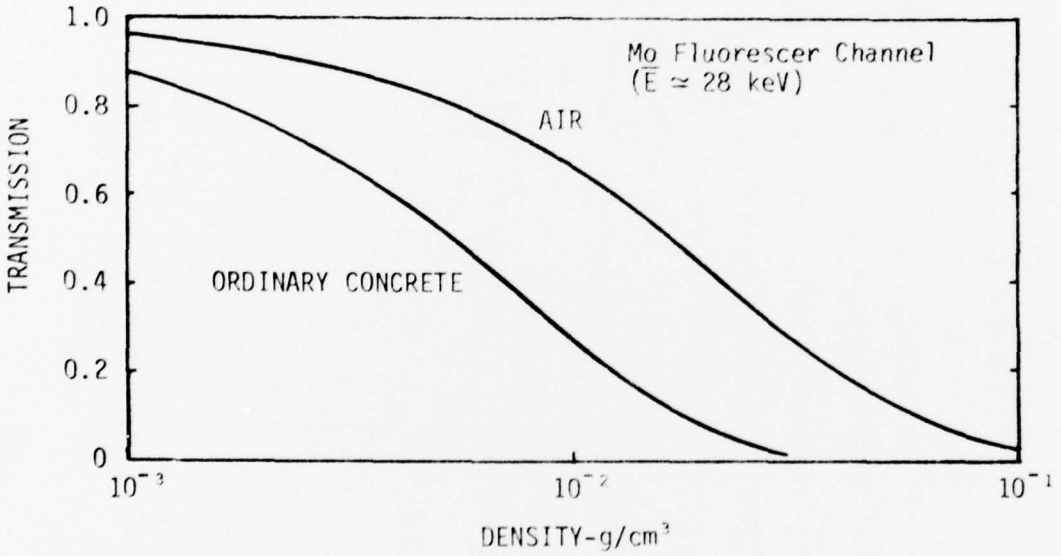

Figure 2.7. Transmission as a function of material density in a 1 meter pipe for Mo fluorescer channel and W anode tube.

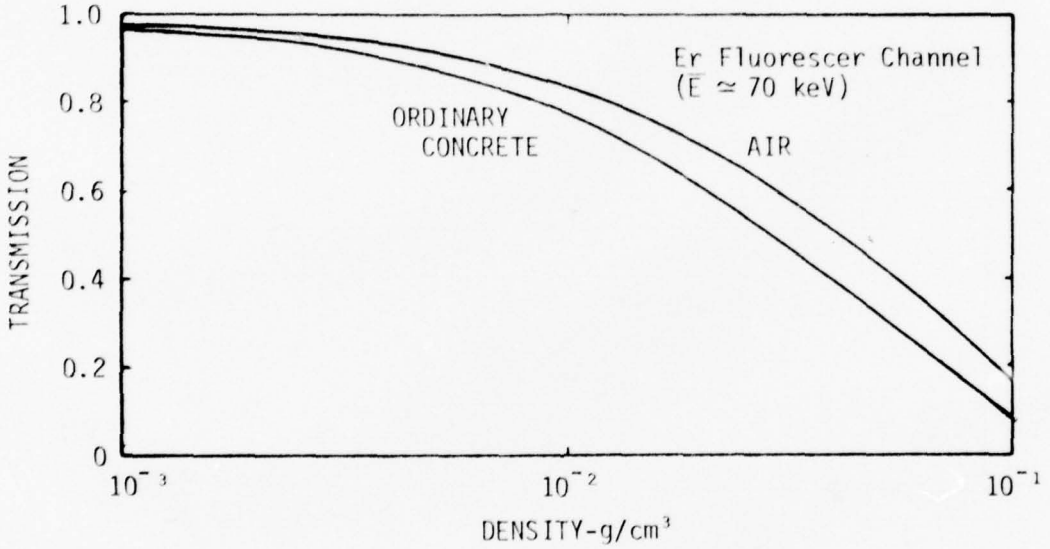

Figure 2.8. Transmission as a function of material density in a 1 meter pipe for Er fluorescer channel.

The unfiltered SSD channel now observes an average energy of just slightly less than 20 keV, being dominated by the x-rays in the molybdenum K lines at 17.8 keV. The molybdenum fluorescer channel observes an average energy of about 25 to 30 eV, as with the tungsten anode tube, and the erbium fluorescer observes a slightly higher average energy of 70 to 80 keV rather than 60 to 70 keV. Figure 2.9 presents x-ray transmission as a function of material density in a 1 meter pipe for the unfiltered SSD channel and a molybdenum anode source. The molybdenum anode source allows one to field response functions which can determine air densities with reasonably accuracy to as low as 2.5×10^{-3} g/cm^3 (corresponding to an 0.8 transmission), an improvement over the 5×10^{-3} g/cm^3 lower limit for the tungsten anode tube.

The unattenuated milliampere signal levels should be adequate to obtain a dynamic range of about two orders of magnitude in the data recording, especially since the 50 to 100 ns pulsed character of the flash x-ray source would allow the signals to be readily resolved from longer time scale components of EMP noise and late time DC offsets in the recording system.

2.4 Line-of-Sight System

The most serious problem to be solved in the fielding of an x-ray attenuation measurement is the construction of a los system that allows x-rays to penetrate the pipe walls, moves radially outward with the walls of the pipe as they are driven by the interior pressure, provides shock isolation for the source and detectors for one or two milliseconds, and does not spall or mechanically fail under peak pressure loading.

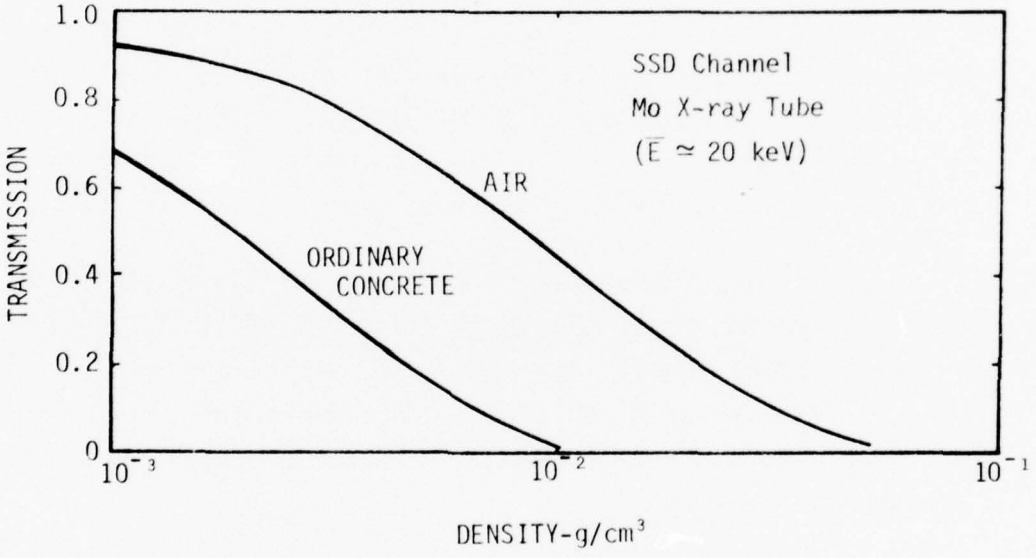

Figure 2.9. Transmission as a function of material density in a 1 meter pipe for SSD channel and Mo anode tube.

Beryllium is the optimal material to use for the x-ray transmitting windows in the sides of the shocked pipe, since it is the lowest atomic number element (Z=4) with structural rigidity and strength. It hence combines the properties of minimum x-ray attenuation with maximum structural strength for any given material thickness.

Kawecki Berylco Industries is the major fabricator of beryllium with the required structural qualities. Their plate grade beryllium, PR-20, is made by cross rolling beryllium block produced by the hot pressing of beryllium powder. The ultimate tensile strength of this material is 60,000 psi, the yield strength (0.2% offset) is 45,000 psi, and the elongation about 3%. These values are typical of the ultimate mechanical properties of high strength, high purity beryllium in block, plate and extruded form.

Calculations have been performed for a high pressure front moving parallel to the beryllium surface. Spall of the rear surface is calculated to occur for pressures in excess of 4 kilobars.

Calculations have also been performed on the survivability of a beryllium plate of thickness t positioned over a long thin slot of width w. A number of separate approximations were made to reduce the calculation to various textbook cases:

i) Thin plate ($w \gtrsim 4t$) with simply supported edges;

ii) Thin plate ($w \gtrsim 4t$) with fixed edges;

iii) A thick inscribed cylinder supported to provide maximum strength;

iv) A thick superscribed cylinder supported to provide maximum strength.

These four cases are sketched in Figure 2.10. The thick cylinder configurations allow one to estimate the fail level for an optimally supported flat plate by comparing it to a cylinder with the proper ratio of wall thickness to diameter.

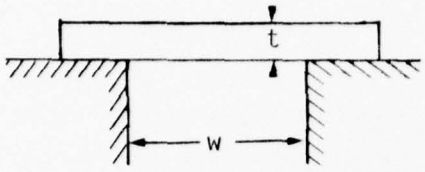

Model 1. Thin plate, $w \gtrsim 4t$, simply supported edges.

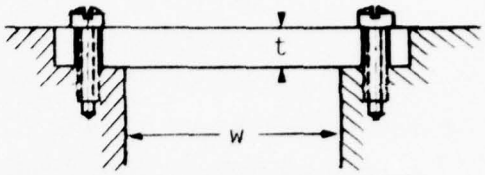

Model 2. Thin plate, $w \geq 4t$, fixed edges.

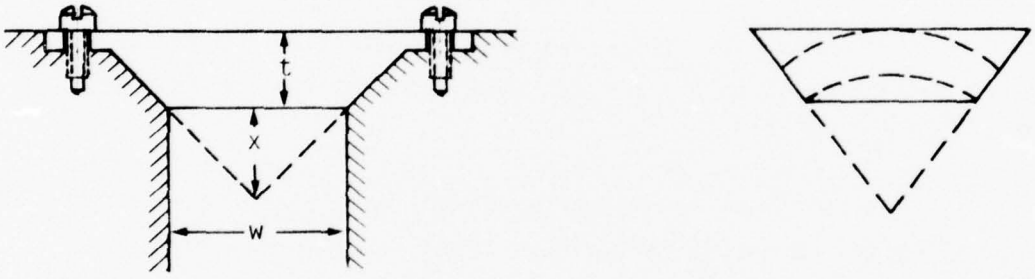

Model 3. Strongest inscribed cylinder, $x = (w/2)^2 t$

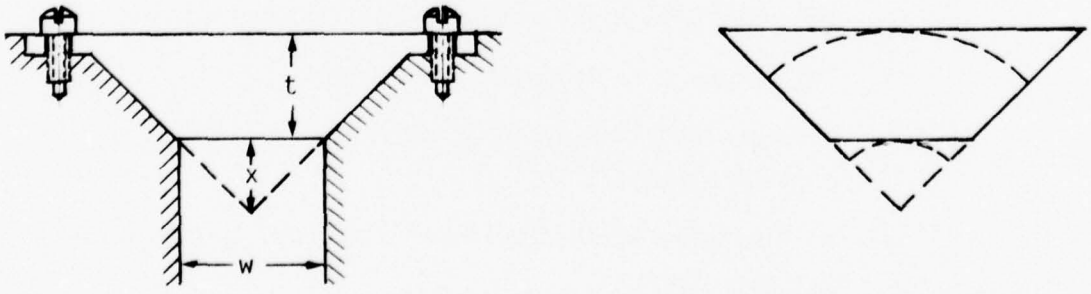

Model 4. Strongest superscribed cylinder, $x = (w/2)t$

Figure 2.10. Beryllium support geometries for various calculational models.

Figure 2.11 presents the results for these four separate cases. Both thick cylinder models give the same results for w/t = 0 or an infinitely thick plate. Beryllium goes plastic at a static pressure greater than 30 kpsi or 2.1 kbars, equal to half its ultimate tensile strength. For a more representative value of w/t = 1, corresponding to a one inch thickness of beryllium over a one inch wide slot, beryllium fails at a pressure of about 1.75 kbar. For a value for w/t greater than 2, all four models are in essential agreement, thus confirming the accuracy of the calculational approximations.

It thus appears that beryllium is unable to withstand static pressures in excess of two kilobars, although under dynamic loading the fail pressures will undoubtedly be higher. A slot geometry has been assumed so that a linear array of flash x-ray tubes may all be pointed at a single detector aperture. The slot would be alined with the axis of the pipe so that any slight translational motion in the window would not remove the beryllium from the source-detector los. A one inch beryllium thickness and slot width was assumed for the calculations of Section 2.3, resulting in the window x-ray transmission as a function of energy presented in Figure 2.12. A thicker window would result in signal levels of less than a milliampere and not enhance significantly the failure strength of the window assembly. A thinner window would significantly compromise the window survivability for a slot of one inch width as required for milliampere signal levels.

The 2 kbar limit for beryllium failure under static loading, coupled with the 4 kbar level for spall, necessitate fielding the transmission measurement at relatively low peak pressures of a few kilobars. Predicted peak pressures in this range occur towards the rear of the 3 foot concrete pipe beyond 80 meters, as shown in Figure 2.13.

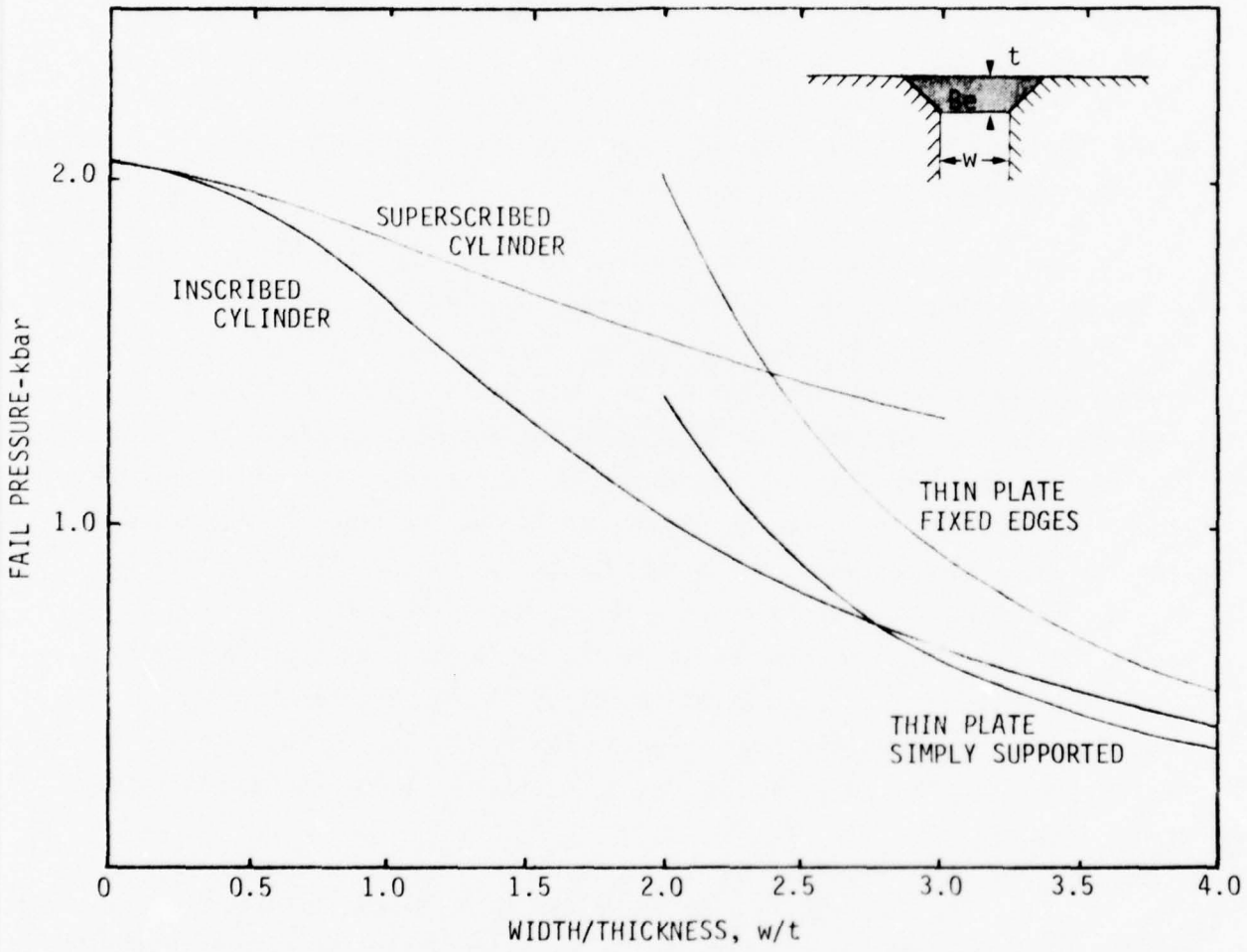

Figure 2.11. Calculated fail pressure for beryllium x-ray window.

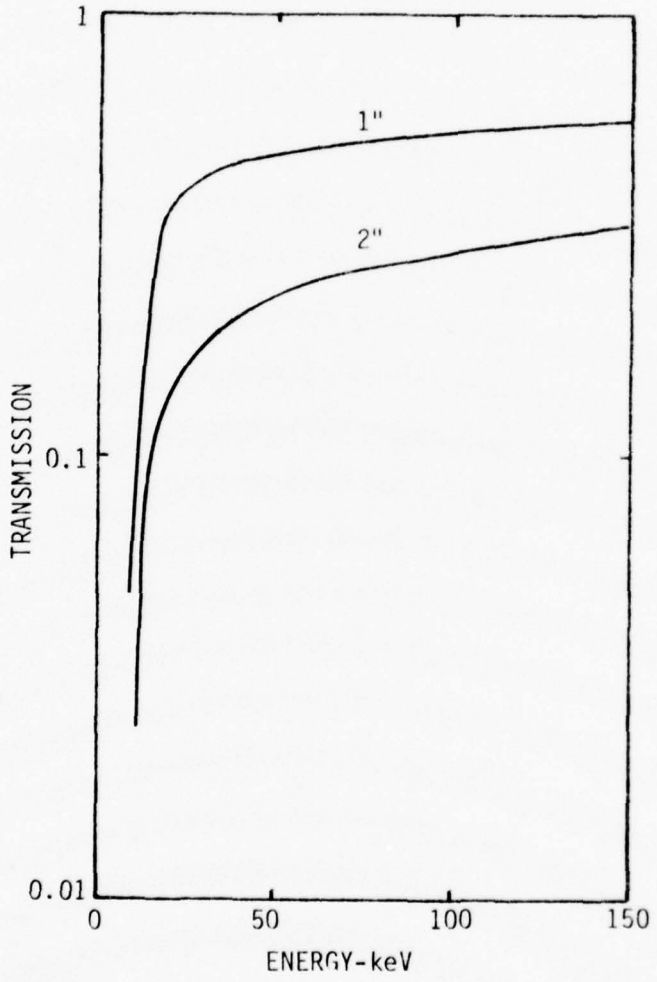

Figure 2.12. X-ray transmission through beryllium windows.

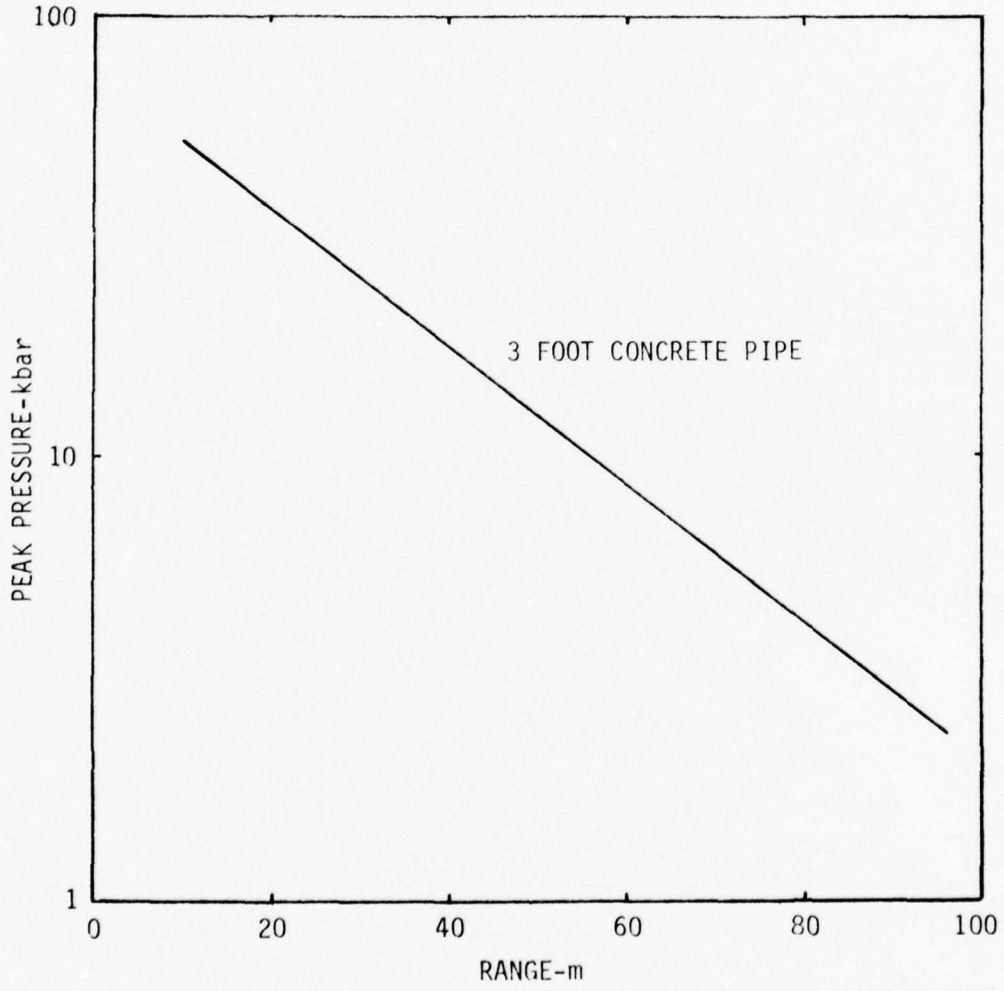

Figure 2.13. Peak pressure versus range in a 3 foot concrete pipe.

Figure 2.14 presents the results of calculations for the radial outward movement of the three foot diameter pipe wall driven by the internal pressures. Towards the rear of the pipe, radial wall velocities are on the order of 20 cm/ms, so that significant increases in the attenuation path length across the pipe occur in the millisecond time scale of the measurement. It is necessary for the beryllium window assemblies to move outward with the wall, lest they stick into the flow, perturb it, and are either eroded away or physically displaced as a result.

Figure 2.15 presents a conceptual design for a window support system. The beryllium window is supported on a steel plate of adequate thickness and strength to span a void area of adequately large diameter that material will not move into the los in the desired measurement time on the order of a millisecond. The velocity, V_g^f, of a free grout surface being driven by a shock pressure p in the grout is given by

$$V_g^f = 2U_g \tag{2.8}$$

where $U_g = \frac{p}{\rho c_g}$ is the material velocity in the grout,

c_g is the grout sound speed (0.2 cm/μs)

and ρ is the grout density (2 g/cm^3)

For a driving shock pressure of 5 kbars (5 x 10^9 dynes/cm^2),

$$U_g = 12.5 \text{ cm/ms}$$

$$V_g^f = 25 \text{ cm/ms}$$

Hence a 60 cm diameter void area would be required to assure that no shocked grout entered the los in a millisecond. The inner diameter of the grout is lined with aluminum or steel to prevent spall.

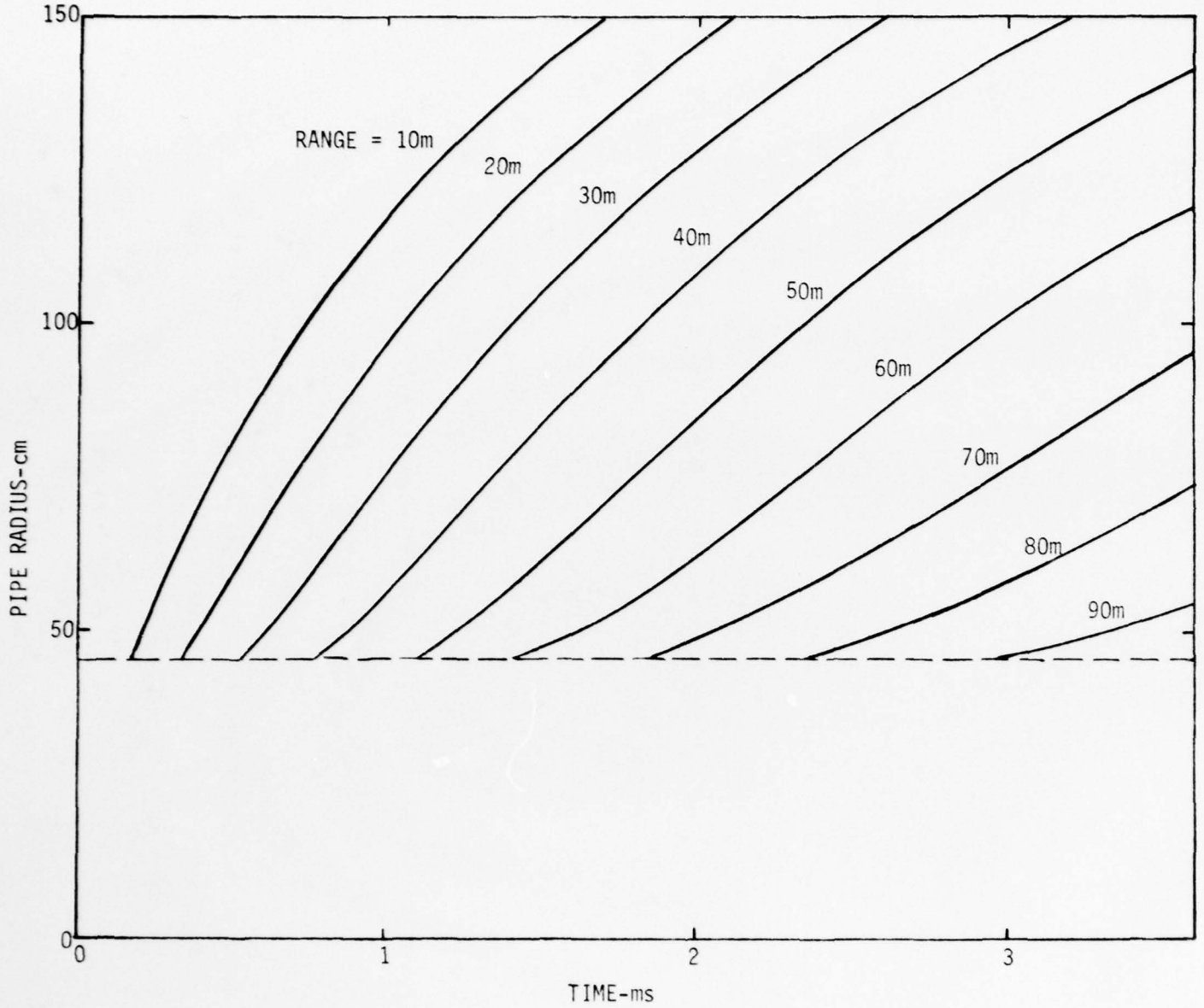

Figure 2.14. Outward movement of 3 foot diameter concrete pipe wall as a function of time and range.

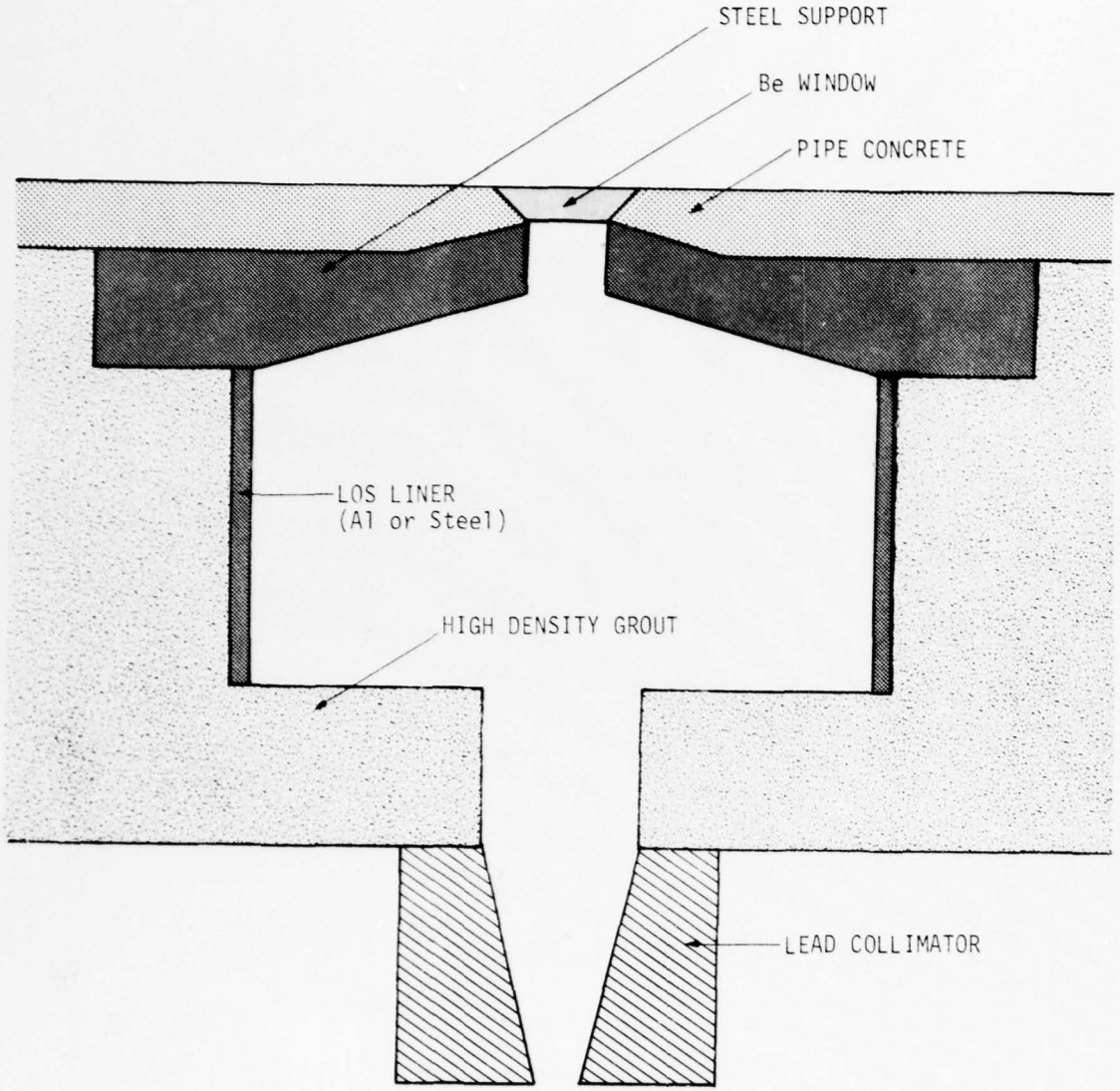

Figure 2.15. Conceptual design for window support system.

It is evident that the construction of a suitable window assembly system is the most serious problem yet to be resolved in the design of an x-ray attenuation measurement to determine shocked material densities in the kilobar regime. The simple calculations already performed are probably conservative in indicating window failure above a few kilobars. The radial motion of the window is probably a more serious problem and more sophisticated calculations would have to be done to design a window and support assembly which would move outward with the pipe wall. Calculations would have to be performed with 2-D hydrodynamic codes to validate a proposed design and to indicate necessary modifications. In addition, a high explosive testing program should be undertaken to proof test the window assembly prior to final application in the field.

2.5 Background Calculations

Calculations have been performed to assure that the neutron and gamma induced background levels are safely less than the predicted milliampere signal levels in a typical fielded configuration. The prompt gamma background from the device occurs at zero time, whereas the x-ray attenuation signals are not recorded until two or three milliseconds later. Thus the initial prompt gamma pulse can only perturb the attenuation measurement if it generates a signal level which saturates the detector or recording system so that either has not adequately recovered by signal time a few milliseconds later.

Calculations of the Hybla Gold radiation environments have been performed by SAI under DNA Contract 001-77-C-0201 and were used in calculating the induced background levels.

The late time background will result from thermalized neutrons and gammas generated from thermal neutron capture. For times greater than a millisecond, these background levels are calculated to be down more than four orders of magnitude from the prompt gamma dose and hence should not be a significant problem.

The peak gamma dose in the center of the three foot pipe at 80 meters from the pipe mouth was calculated to be 3.5×10^9 rads/s and to persist for about 10^{-7} second. The thermal capture dose at times greater than a millisecond was calculated to be less than 10^6 rads/s. The reduction in dose as a function of distance from the pipe wall is significant, being down about an order of magnitude at the wall itself, down at least four orders of magnitude three feet from the wall at the position of the SSD detectors, and down at least five orders of magnitude four feet from the wall at the position of the scintillator-photomultiplier detectors.

The resulting prompt gamma background signal induced in a 300 μm thick SSD three feet back from the pipe wall is about 50 mA/cm^2 of detector area. Two inches of lead surrounding such a detector reduces this background level about two orders of magnitude to about a milliampere, comparable with the predicted x-ray signal levels. The late time background will be down three or four orders of magnitude from this level and hence will be insignificant.

Gammas can also scatter to the detectors from material in the collimated los through the pipe. Assuming a five inch diameter viewed area at three feet from the detector and a peak gamma dose at the pipe wall an order of magnitude down from the value in the middle of the pipe, a signal level of about 50 mA/cm^2 is again obtained for a SSD, comparable to the above unshielded value from prompt gammas diffusing out from the wall.

Similar calculations can be done for a scintillator-photomultiplier detector. A typical plastic scintillator as NE-102 coupled to a 10^6 gain photomultiplier with a sensitivity of 60 A/lm has a combined sensitivity of about 100 coulomb/joule (absorbed in scintillator). For a 2 inch diameter PM tube and a lead or tin loaded plastic scintillator, the background signal from prompt gammas present four feet out from the pipe wall is about 3×10^3A. About 8 inches of lead are required to provide at least five orders of magnitude attenuation so that PM tube outputs are kept safely below an ampere. The background levels at shock arrival time would then be safely less than 0.1 mA relative to a nominal 10 mA signal level. Higher current levels would perturb the dynode voltages in the PM tube divider string so that output linearity at later times would be affected.

The background signal from prompt gammas scattering into the fluorescer los and then scattering from the fluorescer to the scintillator is about 10 mA.

According to the above calculations the background levels at shock arrival time should be at least two orders of magnitude less than the predicted signal levels. The prompt gamma background in the PM tube might be as large as a few tens of milliamperes but the duration of this signal is sufficiently short that the voltages in a properly designed divider string will not be significantly perturbed.

3. HYBLA GOLD EXPERIMENTAL PROGRAM

3.1 Experimental Configuration

In order to verify the feasibility of an x-ray attenuation measurement from the standpoint of detector background levels and equipment survivability, a minimal effort was fielded in conjunction with the SLA "rho flow" experiment positioned on the three foot concrete pipe 83 meters from the zero room wall. A silicon solid state detector was fielded about three feet from the pipe observing the pipe wall through a five inch diameter collimated los. A scintillator-PM tube was fielded about four feet from the pipe wall, observing an 0.2 g/cm^2 fluorescer nine inches away that was placed in the five inch diameter collimated los to the pipe wall. Approximately two inches of lead surrounded the SSD, at least eight inches of lead was between the photomultiplier tube and the pipe wall. The experimental layout is shown in Figure 3.1.

The purpose of this effort was to verify the background levels calculated in Section 2.5 and to ascertain if the detectors and cabling would survive a millisecond or two through groundshock. Since sound and shock speed in tuff and grout at a few kilobars is a few meters per millisecond, it was necessary for the detectors and cables to survive the initial ground shock driven radially outward from the pipe by the air shock moving through it if the detection system were to survive for the one or two milliseconds required to determine the shocked flow conditions in the pipe.

No x-ray source was fielded; x-ray transmitting windows were not placed in the pipe wall; no los protection system was fielded to keep open the x-ray path to the detectors; and no special effort was taken to shock mount the detectors other than to surround the PM tube with a quarter inch of styrofoam. Adequate gamma shielding was placed around the detectors, which were otherwise configured as they would be in an actual measurement.

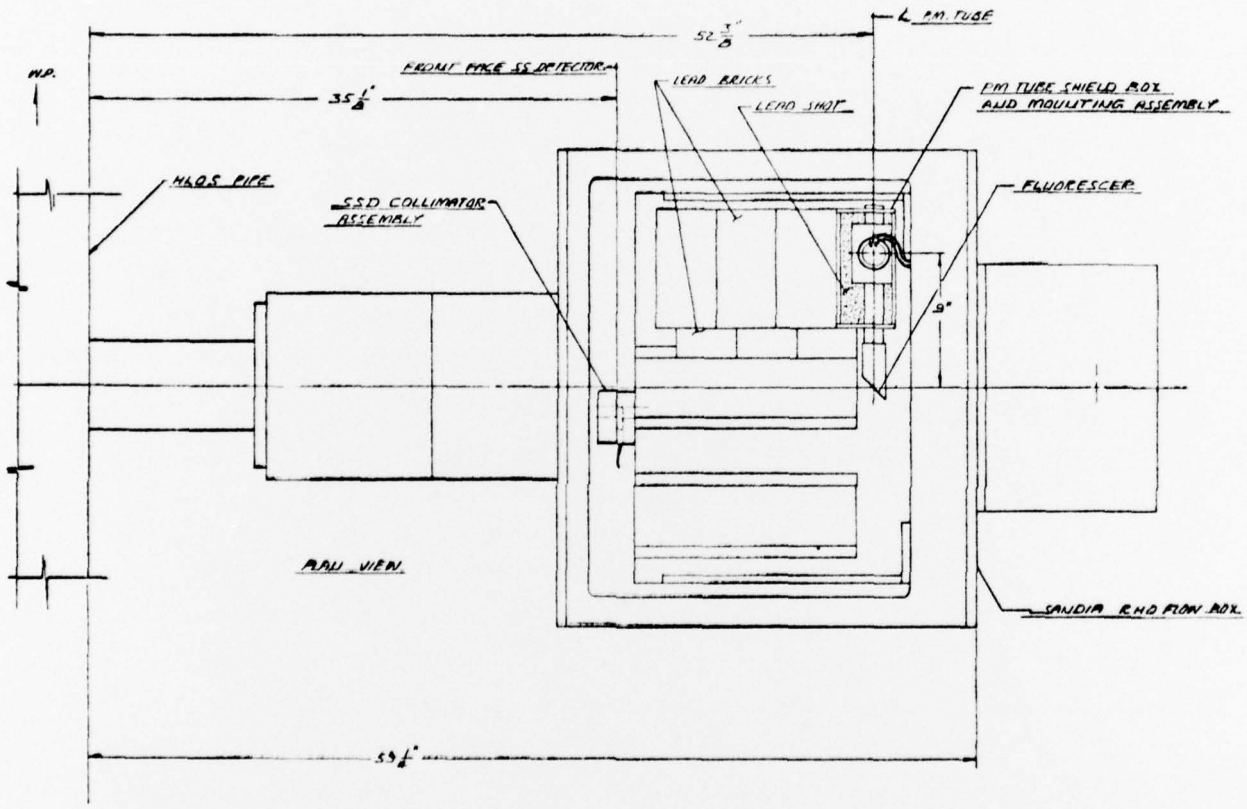

Figure 3.1. Experimental configuration for Hybla Gold feasibility channels.

The solid state detector was an Ortec totally depleted surface barrier detector 300 μm thick and 3 cm^2 in area (Model TB-018-300-300), mounted in a transmission mount and biased 200 V positive. The scintillator was a two inch diameter by one inch thick piece of Ne 102. The photomultiplier tube was an Amperex XP2008 with 1½ inch diameter and 60 A/lm sensitivity (10^6 gain) at its fielded voltage of 1.5 kV.

The PM tube voltage divider string was designed to provide response linearity to 200 mA with a 2.5 ns pulse rise time and 5 ns duration, suitable for recording the predicted few milliampere signal levels of 100 ns duration. Capacitances across the last dynode stages and a one milliampere string current were chosen so that the predicted signal and background levels would not produce greater than a one percent change in the dynode voltages, as required to maintain stable gain to within a percent.

3.2 Recording System

Three channels were fielded: one observing the SSD output, one observing the photomultiplier output, and one an instrumented cable to the "rho flow" box with an open termination. The high voltage (-1.5kV) cable to the PM tube shorted out soon after button up. As a result, the PM signal was not indicative of the background observed by a high gain detector but only of cable and detector survivability.

The recording system was set to record on a single oscilloscope successively displaced multiple sweeps of 0.5 μs duration initiated every 0.5 ms, as would be required to record the output of successively triggered flash x-ray machines generating pulses of 0.1 μs duration. A 30 ns pulse was periodically sent down the cable just prior to each recording interval. The reflection of this pulse from the effectively open termination at the detector was recorded. The shape and polarity of the reflected pulse was indicative of the state of the cable and detector at the time the test pulse arrived, since a shorting of the cable or detector would invert the reflected signal.

A second oscilloscope recorded a 10 μs time window from -2 to +8 μs about zero time in order to observe the prompt gamma and high energy neutron induced background signals.

High pass filters to block signal components below about 1 MHz were installed at the recording trailer to minimize any baseline offset caused by anomalous cable charging on the millisecond time scale. Since the signals to be observed were of less than 0.1 μs duration, the recording system was designed to discriminate against longer time scale background effects resulting either from neutrons or anomalous cable charging effects.

The recording system was equalized to 20 MHz, corresponding to a 20 ns risetime. The HP 180 recording oscilloscopes operating at 1 μs/division were only marginally capable of recording such a rapid signal risetime, comparable with the risetime of the predicted prompt gamma pulse of about 100 ns duration.

The detector signals were routed approximately 300 feet to a signal conditioning alcove through RG-22B/U twinaxial cable. The detectors were connected between one of the center conductors and the cable shield. The second center conductor was left floating in close proximity to the detector. The two RG-22B/U center conductors were connected through DC isolating capacitors to a balun transformer with a grounded centertap, which served to reject common mode noise coupled to the center conductors with respect to the shield. The single-ended output of the balun converted the 92 ohm RG-22B/U signal impedance to the 50 ohm impedance of the 5000 foot long RG-331 cable which carried the signal from the alcove to the recording trailer on the mesa.

3.3 Results

The SSD channel observed a background signal at prompt gamma arrival time of 1.2 mA magnitude and 100 ns duration. Prompt gamma background was predicted to be about 1 mA from the gamma level calculated to exist three feet from the pipe wall, about 100 mA from gammas scattered by the pipe wall in the detector line-of-sight. The failure to observe the 100 mA scattered gamma signal is probably indicative of shadowing of the pipe wall by forward sections of pipe.

A second well defined background signal component of 5 mA magnitude and 200 ns duration occurred 1.4 μs after prompt gamma time. Predicted background levels at this time were an order of magnitude down from the prompt gamma peak and corresponded to 14 MeV neutron arrival time. No measurable background was observed beyond 2 μs. The magnitude of this second component is unexplained but not large enough to compromise the later time signal recording.

The multiply swept oscilloscope records observed no background effects on the millisecond time scale. The reflected test pulse was nominal through 3.5 ms but was indicative of a shorted detector or detector jumper cable on the 4 millisecond sweep. The detector and cabling were thus verified to have remained intact for at least 3.5 ms, allowing about a one millisecond recording window after air shock arrival observed by separate SLA instrumentation in the rho flow box to have occurred at 2.75 ms, essentially as predicted. The peak pressure in the pipe was observed by S^3 to be about 1.3 kbar at 84.5 meters, about half as great as predicted.

The PM background channel observed no measurable background and there was no perturbation of the reflected test pulse over the 5 ms recording period for the multiply swept oscilloscope record.

From the standpoint of background and detector survivability, the minimal effort fielded on Hybla Gold has confirmed the feasibility of an x-ray attenuation measurement of material density in a pipe carrying a few kilobar air shock.

4. CONCLUSIONS

An x-ray attenuation measurement has been conceptually designed to determine the time-dependent density and composition of material in a shock driven pipe at pressures in excess of a kilobar.

Field-emission type x-ray generators are required to produce adequate signal levels. These x-ray sources would be pulsed sequentially at intervals of a few tenths of a millisecond to obtain a series of snapshots of the shocked flow. The pulsed (100 ns duration) character of the x-ray source would result in signals that could be readily observed in the presence of detector dark currents, gamma and neutron induced backgrounds, long time scale components of EMP noise and late time voltage offsets in the recording system.

The detection system is composed of both silicon solid state detectors directly viewing the source and adequately shielded scintillator-photomultiplier detectors observing x-ray irradiated fluorescers. The direct viewing solid state detectors observe an average energy of 25 keV with a tungsten anode source, just under 20 keV with a molybdenum anode source, lower energies being attenuated by the roughly two inches of beryllium required for x-ray transmitting windows on either side of the pipe, higher energies not being absorbed in the relatively thin silicon detectors. The fluorescer/scintillator-photomultiplier detection technique observes energies as low as 25 keV with a molybdenum fluorescer, as high as 70 keV with an erbium fluorescer, there not being sufficient source output to generate significantly higher energy response. Signal levels of a few milliamperes are achievable with either detection technique in a realistic experimental configuration. The energy response of two or three such detector channels is capable of distinguishing air from ablated pipe wall material at densities of from 10^{-3} to 10^{-1} g/cm^3 in one and three foot diameter pipes with typical accuracies of at least 20 percent.

Gamma and neutron induced backgrounds have been calculated to produce manageable prompt background levels comparable with predicted signal levels in adequately shielded detectors, negligible background levels at shock arrival time milliseconds later.

The most serious problem still to be solved is the construction of a los protection system which moves radially outward with the walls of the shock driven pipe, provides shock isolation for the source and detectors for a few milliseconds and does not introduce significant x-ray attenuating material into the los. A tentative design for this system has been formulated, but calculational verification and high explosive testing would be required to validate the concept prior to final application in the field. Calculations made to determine the survivability of beryllium x-ray windows for both static loading and spall infer failure at pressure levels in excess of a few kilobars, thus necessitating the placement of the x-ray attenuation experiment at the rear of the shock driven pipes.

A minimal experimental effort was fielded on Hybla Gold to verify background level calculations and to ascertain if the detectors and close-in recording system would survive the millisecond or two required to determine the shocked flow conditions in the pipe. Gamma and neutron induced backgrounds were observed to be of manageable level and were consistent with calculation. There was no trace of any anonalous signal perturbation of milliampere magnitude at shock arrival time. The detector survivability experiment indicated a shorting of the solid state detector or its jumper cable three feet from the pipe wall about a millisecond after peak shock arrival. An instrumented photomultiplier tube positioned four feet from the pipe wall gave no indication of detector failure through two or three milliseconds after shock arrival.

DISTRIBUTION LIST

DEPARTMENT OF DEFENSE

Defense Documentation Center, Cameron Station
12 cy ATTN: TC

Defense Nuclear Agency
ATTN: STVL
ATTN: RAEV
ATTN: DDST
2 cy ATTN: STSP
4 cy ATTN: TITL

Field Command, Defense Nuclear Agency
ATTN: FCTMOF
ATTN: FCPR
ATTN: FCTMD
ATTN: FCTMC

Field Command Test Directorate
Test Construction Division
ATTN: FCTC

Livermore Division, Fld. Command, DNA
ATTN: FCPRL

Under Sec'y of Def. for Rsch. & Engrg.
ATTN: Strategic & Space Systems (OS)

Assistant to the Secretary of Defense, Atomic Energy
ATTN: Executive Assistant

DEPARTMENT OF THE ARMY

Assistant Secretary of the Army
Research and Development
ATTN: Assistant Secretary for R&D

Deputy Chief of Staff for Rsch. Dev. & Acq.
ATTN: DESRADA/CSM/N

Harry Diamond Laboratories
ATTN: DELHD-NP

U.S. Army Engr. Waterways Exper. Sta.
ATTN: J. Day
ATTN: F. Hanes

DEPARTMENT OF THE NAVY

Assistant Secretary of the Navy
Research and Development
ATTN: Assistant Secretary for R&D

Naval Surface Weapons Center
ATTN: Code F31

Office of the Chief of Naval Operations
ATTN: OP 981

DEPARTMENT OF THE AIR FORCE

AF Weapons Laboratory, AFSC
ATTN: NT/Col Wheeler
ATTN: SUL
ATTN: D. Ray
ATTN: ELP/W. Page
ATTN: DYM/C. Rhoades, Jr.

DEPARTMENT OF THE AIR FORCE (Continued)

Assistant Secretary of the Air Force
Research and Development
ATTN: Assistant Secretary for R&D

Deputy Chief of Staff
Research and Development
ATTN: AF/RDQSM

Space and Missile Systems Organization/MN
Air Force Systems Command
2 cy ATTN: MNNH

DEPARTMENT OF ENERGY

Nevada Operations Office
ATTN: Doc. Con. for Technical Library

Lawrence Livermore Laboratory
ATTN: Doc. Con. for Technical Information
Dept., Library

Los Alamos Scientific Laboratory
ATTN: Doc. Con. for J. McQueen
ATTN: Doc. Con. for ADWP/FCDNA
ATTN: Doc. Con. for Reports Library
ATTN: Doc. Con. for D. Eilers
ATTN: Doc. Con. for C. Keller

Sandia Laboratories
Livermore Laboratory
ATTN: Doc. Con. for Library & Security
Classification Div.

Sandia Laboratories
ATTN: Doc. Con. for C. Broyles
ATTN: Doc. Con. for S. Dolce
ATTN: Doc. Con. for Technical Library Dept.
ATTN: Doc. Con. for J. Kennedy
ATTN: Doc. Con. for J. Plimpton
ATTN: Doc. Con. for P. Nelson

DEPARTMENT OF DEFENSE CONTRACTORS

Electromechanical Sys. of New Mexico, Inc.
ATTN: R. Shunk

General Electric Co.-TEMPO
Center for Advanced Studies
ATTN: DASIAC

H-Tech Laboratories, Inc.
ATTN: B. Hartenbaum

JAYCOR
ATTN: L. Scott

Kaman Sciences Corp.
ATTN: H. Hollister
ATTN: W. Rich
ATTN: F. Shelton

Merritt CASES, Inc.
ATTN: J. Merritt

DEPARTMENT OF DEFENSE CONTRACTORS (Continued)

Mission Research Corp.
ATTN: C. Longmire
ATTN: V. Van Lint

Pacifica Technology
ATTN: G. Kent

Physics International Co.
ATTN: J. Kochley
ATTN: C. Vincent

R & D Associates
ATTN: C. Knowles
ATTN: R. Poll
ATTN: Technical Information Center
ATTN: J. Stockton

Science Applications, Inc.
ATTN: R. Parkinson

Science Applications, Inc.
ATTN: R. Miller

DEPARTMENT OF DEFENSE CONTRACTORS (Continued)

Science Applications, Inc.
ATTN: K. Sites

SRI International
ATTN: D. Keough

Systems, Science & Software, Inc.
ATTN: C. Dismukes/H. Krate/P. Coleman

TRW Defense & Space Sys. Group
ATTN: P. Lieberman

Acurex Corp.
ATTN: J. Huntington

Artec Associates, Inc.
ATTN: D. Baum

Tech Reps Inc.
ATTN: R. Holmes